Factor-Three-Coarsening Nonsymmetric Black Box Multigrid

Marion Bendig* Irad Yavneh†

January 2011

Abstract

The classical Petrov-Galerkin approach to Black Box multigrid for nonsymmetric problems due to Dendy is combined with the recent factor-three-coarsening Black Box algorithm due to Dendy and Moulton, along with a powerful symmetric line Gauss-Seidel smoother, resulting in an efficient and robust multigrid solver. Focusing on the convection-diffusion operator, the algorithm is tested and shown to achieve fast and reliable convergence with both first-order and second-order accurate upstream discretizations of the convection operator for a wide range of diffusion coefficients. The solver also exhibits robust behavior with respect to discontinuous jumps in the diffusion coefficient, and performs well for recirculating flows over a wide range of diffusion coefficients. The efficiency of the solver is supported by results of an analysis for the case of constant coefficients.

1 Introduction

Multigrid computational methods for linear systems of equations arising from the discretization of differential equations are often classified as either "geometric" or "algebraic". The former typically require a highly structured grid and the equations are rediscretized on the coarse grids in order to obtain appropriate operators, while the latter typically ignore the existence of any grid or structure and exploit only the information available in the fine-grid matrix. Nevertheless, intermediate methods have existed for many years. One such approach is the classical Black Box multigrid due to Dendy [8], which is based on the pioneering work of Alcouffe et al. [1]. This approach is designed for a Cartesian grid, and in this sense its generality is limited. However, the prolongation and restriction operators are dependent on the operators, and the coarse-grid operators are constructed algebraically using the Galerkin formalism. This allows the Black Box algorithm to robustly handle symmetric diffusion problems with discontinuous coefficients.

In the last fifteen years or so, a large portion of the research in multigrid methods has shifted towards purely algebraic methods that are applicable to unstructured problems. Recently, however, multigrid algorithms for semi-structured grid have been recommended and are attracting significant interest, e.g., [3, 13]. This trend is associated with hardware development in the last few years, as a result of which, on the one hand, the toll paid in terms of wall-clock time for fully unstructured multigrid is relatively more significant, whereas, on the other hand, the problems that can be solved are so huge that their geometry is well-resolved on grids that are quite coarse compared to the fine resolution that is employed to accurately

*Technische Universität München, bendig@in.tum.de

†Technion—Israel Institute of Technology, irad@cs.technion.ac.il

capture the underlying physics. This leads to multigrid algorithms in which the coarsest grids are unstructured and adapted to the geometry, while all subsequent refinement is structured (typically rectangular or triangular[1]). These approaches bring back the need for powerful and robust multigrid solvers that remain very efficient by taking advantage of the regular grid structure.

This paper focuses on nonsymmetric problems, specifically convection-diffusion, mainly in the convection-dominated regime. In [9], Dendy developed a nonsymmetric version of the original Black Box algorithm [8], employing a Petrov-Galerkin approach, whereby the restriction is no longer the transpose of the prolongation. This algorithm was mainly aimed at solving convection-diffusion problems. The underlying idea is clearly worthy, but the resulting algorithm was only moderately effective, largely due to the use of the safe but relatively ineffective Kaczmarz smoother. In the nearly thirty years that followed, much effort has been invested in acquiring a better understanding of the difficulties underlying such problems, and many useful insights and algorithms have been developed (see, e.g., [4, 9, 7, 5, 20, 18, 15, 2]). Recently, Petrov-Galerkin approaches for nonsymmetric problems that are also suitable for unstructured grids have been developed [2, 14, 6].

With few exceptions, multigrid methods for structured grids apply coarsening by a factor of two along each coordinate, which is the standard approach for creating a hierarchy of structured grids. However, in certain cases there are good reasons for coarsening by a factor of three rather than two (and, conversely, refining by trisection rather than bisection). In the Peano framework [16, 11], for example, coarsening by a factor of three is an inherent property of the underlying space-tree and therefore of all implemented algorithms. This framework uses the Peano space-filling curve (which induces trisection) for a cache-efficient grid traversal as well as a low-memory space-tree encoding. Another reason may be cell-centered discretization, where coarsening by a factor of three has the advantage that it leads naturally to a nested hierarchy of grids (that is, the coarse-grid cells are naturally defined as the union of fine-grid cells). As pointed out in [10], a nested grid hierarchy is necessary in order to obtain a robust multigrid method with low operator complexity. Recall also that coarsening by a factor of three is natural for smoothed-aggregation algorithms when applied on structured grids.

In this work we combine Dendy's classical Black Box multigrid for non-symmetric problems [9] with Dendy and Moulton's recent Black Box multigrid with coarsening by a factor of three [10]. These techniques are implemented in conjunction with a symmetric line Gauss-Seidel smoother (see, e.g., [12] and references therein) to yield an efficient and reliable solver for convection-dominated as well as diffusion-dominated convection-diffusion equations. In Section 2 we describe the equation and the multigrid algorithm. In Section 3 we summarize some results of an analysis of this algorithm that is given in detail in [19]. Section 4 presents results of numerical tests that demonstrate the accuracy, robustness and convergence behavior of algorithm. In Section 5 we summarize the main achievements and talk about future research.

[1] The Black Box algorithms are also applicable to triangular structured grids

2 Model Problem and Algorithm Description

Our model problem is the two-dimensional convection-diffusion equation, written in flux form as

$$Lu = -\nabla \cdot (\epsilon \nabla u) + (au)_x + (bu)_y = f, \qquad (x,y) \in \Omega, \tag{1}$$

$$u_n = k, \quad \text{or} \quad u = g, \qquad (x,y) \in \partial\Omega. \tag{2}$$

Here, $\epsilon > 0$ is the diffusion coefficient and $a(x,y)$ and $b(x,y)$ are the point-wise convection velocities in the x and y direction, respectively. The given functions $f(x,y)$ and $g(x,y)$ (or $k(x,y)$) are the right-hand side forcing and the boundary condition, respectively, and u_n denotes the derivative of u in the direction normal to the boundary. Our variable is $u(x,y)$, which describes, for example, the concentration of a passive tracer in a fluid. The domain in our numerical examples is $\Omega = [-\frac{1}{2}, \frac{1}{2}] \times [-\frac{1}{2}, \frac{1}{2}]$.

2.1 Discretization and Coarse-Grid Operators

We discretize our problem at the cell-centers of a Cartesian grid, using central differences for the Laplacian (diffusion term) and an upstream discretization for the first derivatives (convection terms). We test both first-order and second-order upstream discretizations, as explained in the next section. We denote by h the mesh size of the discrete problem, $L^h u^h = f^h$. In our discussion h is assumed to be uniform, although in our implementation we allow distinct and variable mesh-sizes in the x and y directions. The coarse-grid operators are constructed using the Petrov-Galerkin method, $L^H = RL^hP$, with $H = 3h$ denoting the coarse-grid mesh size, P the prolongation, and R the restriction operator.

2.2 Prolongation and Restriction

For the prolongation and restriction operators we follow the operator-induced method described in [10], albeit with R not equal to the transpose of P. We distinguish between three types of fine-grid points (see Figure 1): those that are collocated with coarse grid points (called c points), those that lie on coarse grid lines (γ points) and those that lie between the coarse grid lines (ι points).

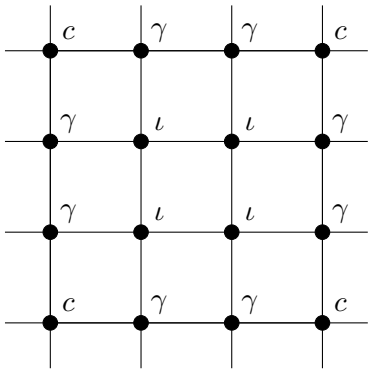

Figure 1: Fine grid point types on the dual grid of cell centers for the Black Box prolongation. Here, c points coincide with the coarse grid.

In the prolongation, each coarse grid point contributes to the 5×5 nearest fine grid points. Conversely, residuals from 5×5 nearest fine-grid points are restricted to the coarse grid. The central value of the prolongation stencil, which corresponds to a c point, is 1 as usual. The weights for the γ points on coarse grid lines are obtained by solving systems of two equations in two unknowns, while the interpolation weights at ι points require solutions of systems of four equations in four unknowns. These linear systems are determined by the fine operator L^h; see [10] for complete details. We also use the following modification advocated in [9, 10]: $u^h \leftarrow u^h + Pu^H + \frac{f^h - L^h u^h}{diag(L^h)}$, i.e., adding the result of a Jacobi step after the prolongation. This generally improves the convergence at a modest cost. Finally, due to our targeting non-symmetric operators, we use the symmetric part of L^h, i.e., $L^h_{sym} = \frac{1}{2}[L^h + (L^h)^T]$, instead of L^h, for the construction of the prolongation and $(L^h)^T$ for the construction of the restriction. This is the approach proposed in [9].

2.3 Relaxation

Instead of using Kaczmarz relaxation, as suggested in [9], we use symmetric X- and Y-Line Gauss-Seidel. By symmetric X/Y-Gauss-Seidel we mean that we go over lines of constant y/x, first in ascending and then in descending x/y direction, and eliminate the residuals along each line simultaneously. This requires solving tridiagonal linear systems. Line Gauss-Seidel or ILU relaxation are commonly used for convection-dominated convection-diffusion problems and for high-Reynolds number flows (see, e.g., [17] and references therein). On the coarsest grid we employ a direct solver.

3 Summary of Analysis Results

An analysis of the non-symmetric Black Box multigrid for the constant-coefficient convection operator is reported in [19]. There it is first shown that any consistent near-neighbor upstream discretization of a 2D convection operator $L = a\partial_x + b\partial_y$ (assuming, without loss of generality, non-negative a and b,) can be written in the form

$$L^h = L^h_0 + c(h) D^h \,, \tag{3}$$

where $c(h)$ is a free parameter,

$$L^h_0 = \frac{1}{2h} \begin{bmatrix} 0 & 0 & 0 \\ -a+b & a+b & 0 \\ -a-b & a-b & 0 \end{bmatrix} \,, \quad \text{and} \quad D^h = \frac{1}{h^2} \begin{bmatrix} 0 & 0 & 0 \\ -1 & 1 & 0 \\ 1 & -1 & 0 \end{bmatrix} .$$

The operator L^h_0 can be interpreted as a second-order accurate discretization of L with respect to the location $(x - \frac{h}{2}, y - \frac{h}{2})$, where (x, y) is the center of the stencil. The operator D^h is a second-order accurate approximation to the mixed second derivative at the same point. This means that (3) can be interpreted as a second-order accurate discretization of the operator $a\partial_x + b\partial_y + c(h)\partial_{xy}$, centered at $(x - \frac{h}{2}, y - \frac{h}{2})$. The term $c(h)\partial_{xy}$ can be considered as an anisotropic artificial diffusion which, for consistency, must vanish as $h \to 0$. Typically, it is the leading-order local truncation term. Note that choosing $c(h) = \frac{1}{2}(a+b)h$ yields the standard first-order upstream stencil. A second interesting choice is $c(h) = 0$, which yields a second-order accurate compact upstream discretization. Note that in this case the operator

contains large positive off-diagonal terms, and yet we shall see that our solver handles this operator quite well.

The nonsymmetric Black Box algorithm for an upstream discretization of the advection operator yields the following prolongation and restriction operators in the constant-coefficient case:

$$P = \frac{1}{9}\begin{bmatrix} 1 & 2 & 3 & 2 & 1 \\ 2 & 4 & 6 & 4 & 2 \\ 3 & 6 & 9 & 6 & 3 \\ 2 & 4 & 6 & 4 & 2 \\ 1 & 2 & 3 & 2 & 1 \end{bmatrix}, \quad R = \begin{bmatrix} 0 & 0 & 0 & 0 & 0 \\ 0 & 0 & 0 & 0 & 0 \\ 1 & 1 & 1 & 0 & 0 \\ 1 & 1 & 1 & 0 & 0 \\ 1 & 1 & 1 & 0 & 0 \end{bmatrix}.$$

In [19] it is shown that these P and R produce a coarse-grid discretization that is a second-order accurate approximation to the fine-grid convection operator. In particular, the relative phase error tends to zero with the mesh-size (c.f. [15]). These operators are of appropriate accuracy for achieving fast convergence with a V cycle (see [18]). In [19] we also analyze line Gauss-Seidel relaxation for the constant-coefficient case. It is shown that if the relaxation is carried out in downstream ordering, then it is a *stable* marching process, which naturally yields an exact solver in the case of pure upstream convection. On the other hand, when it is carried out in upstream ordering (the "wrong" direction) it remains nondivergent. These results hold for any $c(h) \geq 0$. It is also shown that as we appeal to coarser and coarser grids, the relative value of $c(h)$ in the upstream discretization described above tends monotonically to zero. We conclude therefore that symmetric line Gauss-Seidel, whereby line relaxation is carried out in alternating directions, can be expected to yield a robust smoother for this problem, despite the fact that the matrices are not M-matrices. This expectation is borne out in our numerical experiments, including problems with variable coefficients and problems with discontinuous jumps in the diffusion coefficient.

4 Numerical Results

To show the accuracy, robustness, and convergence behavior of our approach, we present numerical results for several scenarios. In all these experiments we use, unless otherwise stated, a V(1, 1) cycle with one symmetric X-line Gauss-Seidel pre-relaxation and one symmetric Y-line Gauss-Seidel post-relaxation. We coarsen down to a 9×9 grid and use a direct solver there. The notation $||.||$ refers to the l_2 norm. We start with a random initial guess and impose a zero right-hand side (which has no effect on the asymptotic convergence behavior of course). The iteration is stopped when the residual norm $||r_i|| = ||f^h - L^h u_i^h||$ is reduced by at least a factor of 10^8. Here, i denotes the iteration number. In addition to the number of iterations needed for reaching this goal, we track the convergence factor ρ, which is defined as $\rho := \frac{||r_i||}{||r_{i-1}||}$. ρ_{mean} stands for the (geometric) mean convergence factor.

4.1 Accuracy

Table 1 (left) displays the accuracy of the discrete solution with $c(h) = 0$ and $c(h) = \frac{1}{2}(a+b)h$ for the convection equation ($\epsilon = 0$), with constant coefficients $a = 1$ and $b = 0.5$. The inflow boundary conditions are $g(-0.5, y) = \frac{(y^2-0.25)^4}{0.25^4}$, and $g(x, -0.5) = 0$, while at the outflow boundaries homogenous Neumann conditions are imposed. We denote by e the difference

between the discrete solution and the exact solution to the differential equation, sampled on the grid, with e_{max} denoting the maximum norm of this error, $||e||_\infty$.

We also check the accuracy for a problem in which a and b depend on the location (x, y). We use $a = 8y(\frac{1}{4} - x^2)$ and $b = -8x(\frac{1}{4} - y^2)$ (see streamlines for the loop-segment problem in Figure 2), imposing the same inflow boundary condition as above at the left-hand boundary, $g(-0.5, y) = \frac{(y^2-0.25)^4}{0.25^4}$, homogeneous Neumann conditions at the outflow boundary, $g(x, -0.5) = 0$, and homogeneous Dirichlet conditions at the remaining two boundaries. For $\epsilon \to 0$, the solution u^h at the outflow boundary should exactly be equal to u^h at the inflow boundary. Therefore we compute $\tilde{e}_{max} = ||u^h_{in} - u^h_{out}||_\infty$ as a measure of accuracy. The results are shown in Table 1 (right).

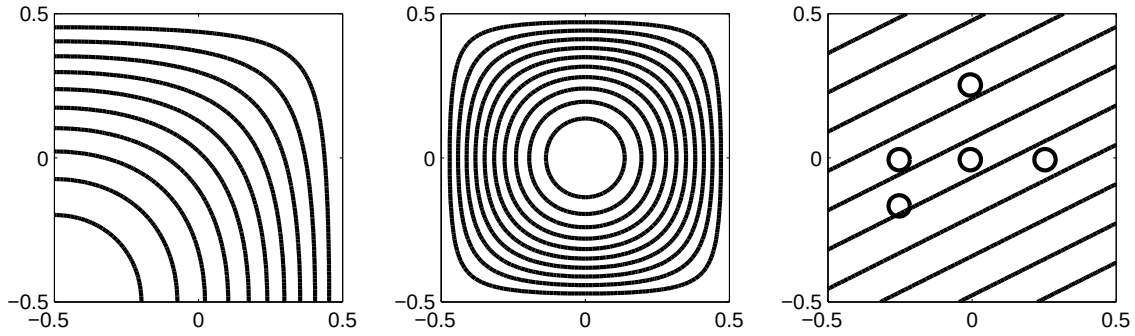

Figure 2: Streamlines for the loop-segment, recirculating-flow, and jumping-diffusion coefficient problems.

For both problems we see that the error with the second-order method, $c(h) = 0$, is almost exactly proportional to h^2, whereas for $c(h) = \frac{1}{2}(a + b)h$ it is proportional to h as expected.

Constant Coefficients		
$\epsilon = 0$, $a = 1$, $b = 0.5$		
$1/h$	e_{max} (1^{st} order)	e_{max} (2^{nd} order)
27	0.2788	0.0108459
81	0.1249	0.0011998
243	0.0466	0.0001337
729	0.0161	0.0000149

Loop Segment		
$\epsilon = 0$		
$1/h$	$\tilde{e}_{max}$ (1^{st} order)	$\tilde{e}_{max}$ (2^{nd} order)
27	0.1587	0.0025276
81	0.0623	0.0002803
243	0.0220	0.0000311
729	0.0075	0.0000035

Table 1: Maximal error for first order $c(h) = \frac{1}{2}(a+b)h$ and second order $c(h) = 0$ discretization.

4.2 Robustness and Efficiency

Constant Coefficients As in the previous section we consider the convection-diffusion equation with non-constant and with constant coefficients. For assessing the convergence behavior we use the geometric-mean convergence factor ρ_{mean}. Figure 3 shows ρ_{mean} as a function of the diffusion coefficient with the first-order and second-order accurate discretizations for various mesh resolutions. For the first-order discretization the convergence factors are uniformly excellent. For the second-order discretization the convergence is still excellent over a wide range of diffusion coefficients, with some deterioration occurring for certain values

of ϵ, which gets worse as the grid is refined. As expected, the convergence rates are excellent in the strongly viscous case, while at the other extreme—the strongly convective regime—the method becomes a stable direct solver.

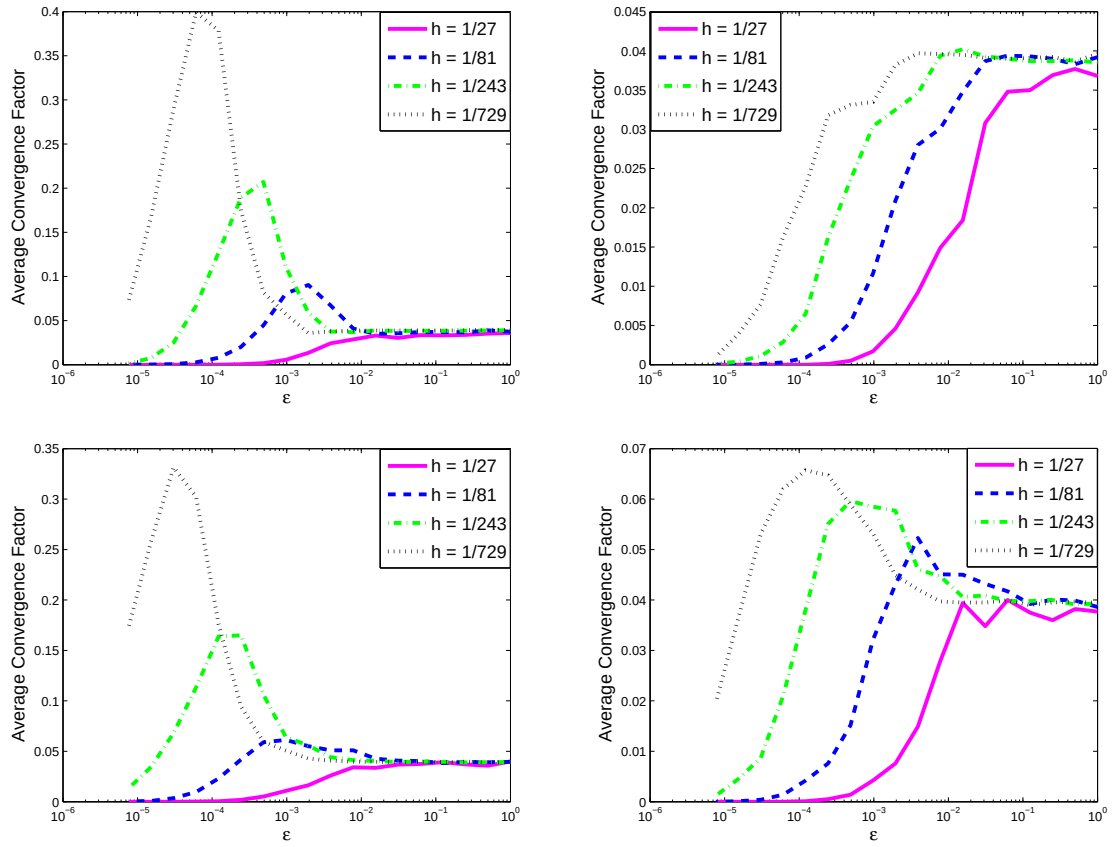

Figure 3: The mean convergence factor ρ_{mean} for the constant coefficient problem (top) with $a = 1$ and $b = 0.5$, and the loop-segment problem (bottom), with $c(h) = 0$ (second order, left) and $c(h) = \frac{1}{2}(a + b)h$ (first order, right).

Jumping Coefficients Next, we introduce jumps in the diffusion coefficient for the constant coefficient case by sharply increasing the diffusion in one or more circular regions (see Figure 2, right, for the streamlines and positions of the jumps). The rest of the setup remains the same as before. Table 2 shows the results for $\epsilon = 10^2$ in one or five circles, respectively, and $\epsilon = 10^{-4}$ in the rest of the domain—a jump by six orders of magnitude. This experiment is motivated by heat flow problems where the property of the conductive material varies in certain regions due to imperfections or embedded materials.

As expected for Black Box methods, the solver appears to be robust. Again, the first-order discretization shows better convergence behavior, however, less significantly so. Interestingly, there is no deterioration with the mesh size for the single-jump case.

Closed Characteristics The next problem that we consider is a flow with closed characteristics, i.e., recirculating flow. We use $a = sin(\pi y)cos(\pi x)$ and $b = cos(\pi y)sin(\pi x)$ and

one jump		
$\epsilon = 10^{-4}[10^2]$, $a = 1$, $b = 0.5$		
$1/h$	# cycles	ρ_{mean}
27	10 (11)	0.145 (0.182)
81	11 (13)	0.187 (0.233)
243	9 (10)	0.121 (0.156)
729	8 (9)	0.093 (0.126)

five jumps		
$\epsilon = 10^{-4}[10^2]$, $a = 1$, $b = 0.5$		
$1/h$	# cycles	ρ_{mean}
27	8 (12)	0.090 (0.208)
81	13 (17)	0.239 (0.323)
243	16 (17)	0.306 (0.332)
729	21 (22)	0.411 (0.426)

Table 2: The constant-coefficient problem with one or five jumps by a factor 10^6 in the diffusion coefficient in circular regions of radii 1/27. The numbers in parentheses show results for the second-order discretization, $c(h) = 0$.

we apply homogeneous Dirichlet boundary conditions on all the boundaries. The streamlines are shown in Figure 2 (middle). The results can be seen in Tables 3 and 4.

The solver yields satisfactory convergence behavior for ϵ down to 10^{-6} for the first-order discretization, and 10^{-3} for the second-order discretization. For $\epsilon = 10^{-4}$ the convergence behavior of the second-order method varies from moderate convergence rates, to slow convergence, and even divergence, depending on the mesh-size. This behavior requires further investigation that is currently under way, and it may be related to various aspects of this problem, in particular, the recirculation, the existence of a stagnation point at the center, and/or loss of stability of the relaxation at very coarse levels. For the first-order discretization, the results are excellent even for small ϵ and very fine grids.

$\epsilon = 10^{-4}$		
$1/h$	# cycles	ρ_{mean}
27	9 (DIV)	0.126 (DIV)
81	11 (>200)	0.180 (0.914)
243	9 (69)	0.125 (0.764)
729	17 (57)	0.331 (0.723)

$\epsilon = 10^{-3}$		
$1/h$	# cycles	ρ_{mean}
27	5 (51)	0.013 (0.697)
81	7 (15)	0.068 (0.283)
243	7 (9)	0.063 (0.126)
729	7 (10)	0.070 (0.151)

Table 3: Convergence rate results for the recirculating flow problem with varying mesh sizes. The numbers in parentheses refer to the second-order discretization. If the method converges slowly we calculate ρ_{mean} after 200 V cycles.

5 Conclusion and Future Work

We presented a multigrid method for solving nonsymmetric problems on a trisected grid by combining Dendy's nonsymmetric Black Box multigrid [9], Dendy and Moulton's Black Box multigrid for trisected grids [10], and a powerful symmetric line relaxation. By choosing the artificial diffusion parameter $c(h)$ as defined in the analysis of [19], we can easily switch between first-order and second-order accurate upstream discretization of the convection operator. The convergence behavior of the method is evaluated and found to be excellent for various scenarios and for first-order as well as second-order accurate discretizations.

We find that even for recirculating flow good convergence behavior is achieved for a wide range of diffusion coefficients. The second-order discretization, which contains large positive off-diagonal terms, shows expectedly slower convergence and less robust behavior in the

$1/h = 243$		
ϵ	# cycles	ρ_{mean}
10^0	6 (6)	0.040 (0.040)
10^{-1}	6 (6)	0.040 (0.040)
10^{-2}	6 (6)	0.045 (0.041)
10^{-3}	8 (9)	0.089 (0.123)
10^{-4}	9 (68)	0.123 (0.762)
10^{-5}	27 (>200)	0.500 (0.941)
10^{-6}	31 (DIV)	0.552 (DIV)
10^{-7}	>200 (DIV)	0.918 (DIV)

Table 4: Convergence rate results for the recirculating flow problem and a range of diffusion coefficient values ϵ. The numbers in parentheses show results for the second-order discretization. If the method converges slowly we calculate ρ_{mean} after 200 V cycles.

convection-dominated recirculating-flow regime, but the overall performance is otherwise excellent. It is hoped that further investigation, currently under way, will yield robust behavior also in the unusual cases where the solver currently fails.

Acknowledgement

The financial support of the International Graduate School of Science and Engineering (IGSSE) of the Technische Universität München under the grant 3.10 is gratefully acknowledged.

References

[1] R. E. Alcouffe, A. Brandt, J. E. Dendy, and J. W. Painter. The Multi-Grid Method for the Diffusion Equation with Strongly Discontinuous Coefficients. *SIAM Journal on Scientific and Statistical Computing*, 2(4):430–454, 1981.

[2] R. E. Bank, J. W. L. Wan, and Z. Qu. Kernel Preserving Multigrid Methods for Convection-Diffusion Equations. *SIAM Journal on Matrix Analysis and Applications*, 27:1150–1171, 2005.

[3] B. Bergen, T. Gradl, U. Rüde, and F. Hülsemann. A Massively Parallel Multigrid Method for Finite Elements. *Computing in Science Engineering*, 8(6):56 –62, 2006.

[4] A. Brandt. Multigrid Solvers for Non-Elliptic and Singular-Pertubation Steady State Problems, 1981.

[5] A. Brandt and I. Yavneh. Accelerated Multigrid Convergence and High-Reynolds Recirculating Flows. *SIAM Journal on Scientific Computing*, 14(3):607–626, 1993.

[6] M. Brezina, T. A. Manteuffel, S. F. McCormick, J. Ruge, and G. Sanders. Towards Adaptive Smoothed Aggregation (AlphaSA) for Nonsymmetric Problems. *SIAM Journal on Scientific Computing*, 32(1):14–39, 2010.

[7] P. M. de Zeeuw. Matrix Dependent Prolongations and Restrictions in a Blackbox Multigrid Solver. *Journal of Computational and Applied Mathematics*, 33:1–27, 1990.

[8] J. E. Dendy. Black Box Multigrid. *Journal of Computational Physics*, 48(3):366–386, 1982.

[9] J. E. Dendy. Black Box Multigrid for Nonsymmetric Problems. *Applied Mathematics and Computation*, 13(3-4):261–283, 1983.

[10] J. E. Dendy and J. D. Moulton. Black Box Multigrid with Coarsening by a Factor of Three. *Numerical Linear Algebra with Applications*, 17:577–598, 2010.

[11] T. Neckel. *The PDE Framework Peano: An Environment for Efficient Flow Simulations.* Dissertation, Institut für Informatik, Technische Universität München, 2009.

[12] C. W. Oosterlee and P. Wesseling. A Robust Multigrid Method for a Discretization of the Incompressible Navier-Stokes Equations in General Coordinates. *IMPACT of Computing in Science and Engineering*, 5:128–151, 1993.

[13] C. Rodrigo. *Geometric Multigrid Methods on Semi-Structured Triangular Grids.* Dissertation, University of Zaragoza, 2010.

[14] M. Sala and R. S. Tuminaro. A New Petrov-Galerkin Smoothed Aggregation Preconditioner for Nonsymmetric Linear Systems. *SIAM Journal on Scientific Computing*, 31:143–166, 2008.

[15] W. L. Wan and T. F. Chan. A Phase Error Analysis of Multigrid Methods for Hyperbolic Equations. *SIAM Journal on Scientific Computing*, 25:857–880, 2003.

[16] T. Weinzierl. *A Framework for Parallel PDE Solvers on Multiscale Adaptive Cartesian Grids.* Dissertation, Institut für Informatik, Technische Universität München, 2009.

[17] P. Wesseling and C. W. Oosterlee. Geometric Multigrid with Applications to Computational Fluid Dynamics. *Journal of Computational and Applied Mathematics*, 128:311–334, 2001.

[18] I. Yavneh. Coarse-Grid Correction for Nonelliptic and Singular Perturbation Problems. *SIAM Journal on Scientific Computing*, 19(5):1682–1699, 1998.

[19] I. Yavneh and M. Bendig. Nonsymmetric Black Box Multigrid with Coarsening by Three: Analysis and Numerical Results. Technical report, Technion Israel Institute of Technology, Haifa, Israel, 2011.

[20] I. Yavneh, C. H. Venner, and A. Brandt. Fast Multigrid Solution of the Advection Problem with Closed Characteristics. *SIAM Journal on Scientific Computing*, 19(1):111–125, 1998.